Dynamics of Competitive Adsorption of Lipase and Ionic Surfactants at the Water–Air Interface

Javadi, A.; Dowlati, S.; Miller, R.; Schneck, E.; Eckert, K.; Kraume, M.;

Originally published:

September 2020

Langmuir 36(2020)40, 12010-1202

DOI: https://doi.org/10.1021/acs.langmuir.0c02222

Dynamics of Competitive Adsorption of Lipase and Ionic Surfactants at the Water–Air Interface

Aliyar Javadi[1, 2, 3, 4], Saeid Dowlati[2], Reinhard Miller[5], Emanuel Schneck[5], Kerstin Eckert[1,4] and Matthias Kraume[3]

1. Institute of Fluid Dynamics, Helmholtz-Zentrum Dresden-Rossendorf (HZDR), Bautzner Landstraße 400, 01328 Dresden, Javadi.aliyar@hzdr.de
2. Chemical Engineering Department, College of Engineering, University of Tehran, 14395-515, Tehran, Iran.
3. TU Berlin, Chair of Chemical and Process Engineering, Straße des 17. Juni135,10623 Berlin, Germany
4. Institute of Process Engineering and Environmental Technology, TU Dresden, 01062 Dresden, Germany.
5. Technical University Darmstadt, Physics Department, 64289 Darmstadt, Germany

Abstract

Lipase is one of the most important enzymes playing a key role in many biological and chemical processes, in particular for fat hydrolysis in living systems and technological applications such as food production, medicine, and biodiesel production. As lipase is soluble in water, the major hydrolysis process occurs at the water–oil interface, where lipase can get in contact with the oil. To provide optimum conditions, the emulsification of the oil is essential to provide a large interfacial area which is generally done by adding surfactants. However, the presence of surfactants can influence the lipase activity and also cause competitive adsorption, resulting in a removal of lipase from the interface or its conformational changes in the solution bulk. Here we have studied the dynamics of competitive adsorption and interfacial elasticity of mixed solutions containing lipase and the anionic surfactant sodium dodecyl sulfate (SDS) or the cationic surfactant cetyltrimethylammonium bromide (CTAB), respectively, at the water–air interface. The experiments were performed with a special coaxial double capillary setup for drop bulk–interface exchange developed for the drop profile analysis tensiometer (PAT) with two protocols: sequential and simultaneous adsorption of single components and mixed systems. The results in terms of dynamic surface tension and dilational visco-elasticity illustrate fast and complete desorption of a pre-adsorbed CTAB and SDS layers via sub-phase exchange with a buffer solution. In contrast, the pre-adsorbed lipase layer cannot be removed either by SDS or CTAB from the interface during drop bulk exchange with a buffer solution due to the unfolding process and conformation evolution of the protein molecules at the interface. In the opposite case, lipase can remove pre-adsorbed SDS and CTAB. The dynamic surface tension and visco-elasticity data measured before and after sub-phase exchange show joint adsorption of lipase and CTAB in the form of complexes, while SDS is adsorbed in competition with lipase. The results are in good correlation with the determined surface charges of the lipase gained by computational simulations which show a dominant negatively charged surface for lipase that can interact with the cationic CTAB while partial positively charged regions are observed for the interaction with the anionic SDS.

Keywords: Surfactant Protein Mixed Adsorbed Layer, Lipase SDS CTAB Complexes and Co-Adsorption, Interfacial Rheology, Enzymatic Reactions at Water-Air Interface.

Graphical Abstract

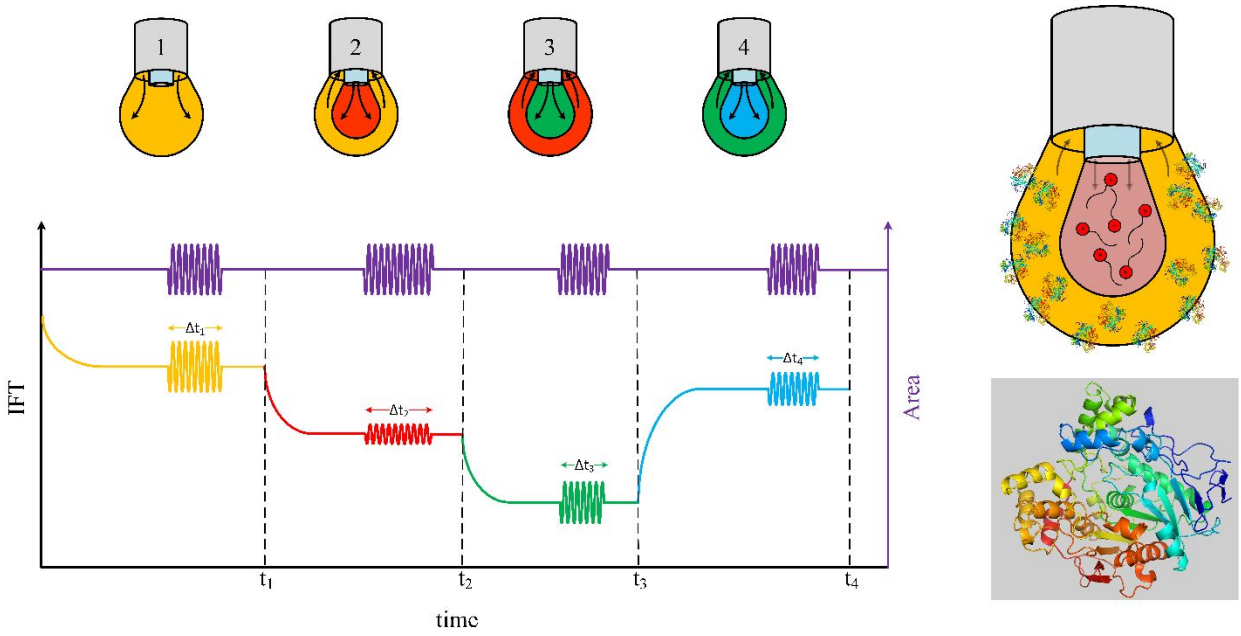

Note: The size of surfactant is exaggagerated compared to the lipase, for the sake of graphical presentation.

1 Introduction

Lipases are proteins that catalyze the process of lipid hydrolysis [1]. In our body, lipase converts triglycerides into fatty acids, simpler glycerides, and glycerol [2]. Lipases are also effective catalyzers for esterification and transesterification reactions [3]. The latter reaction is responsible for the production of biodiesel by breaking animal [4-7], plant [8-12], and waste oil [13-17] into esters of fatty acids [18]. To this aim, lipase biocatalysts have proven their promising environmental benefits over chemical catalysts, e.g., acids and bases, by their reusability, ease of separation, simpler operation, and lower energy requirement; however, high cost of production is their major disadvantage [19-21]. Taken together, owing to their ubiquitous applications, in recent years, lipases received an ever-increasing attention across various disciplines.

Lipase is a hydrophilic protein soluble in water, while lipids are usually hydrophobic [22]. The different polarity between catalyst and substrate in this class of enzymatic reactions brings about the necessity of a heterogeneous reaction, within which reactants should meet and react at the liquid–liquid interface [23]. The catalytic activity of lipase is significantly improved in the interfacial region of oil and water, in comparison with the bulk phases [24]. So, creating a contact region between the immiscible polar and apolar phases, in the form of an emulsion, for instance, can play a significant role in enhancing the reaction rate. Throughout the reaction, characteristics of the interface evolve continually, since different products affect the morphology of the interface, which, in turn, impacts the lipase catalytic behavior [25]. Owing to the interfacial activity, the classic Michaelis–Menten [26] kinetic model cannot be applied to lipases, as their behavior is a function of interfacial excess concentration [27]. In addition to that, the effect of inhibitors, desorption of soluble products from the interface or solubilization of insoluble products by acceptors, or interfacial reorganization and conformational changes should be considered in a quantitative kinetic model [28].

The interfacial behavior of an enzyme is a complex phenomenon that has been the subject of several systematic investigations. Lipase molecules experience an activation after adsorption at interfaces [24]. In many cases, a branched structure of the lipase poses an obstacle, which can be overcome by surface-induced conformational changes in the tertiary structure of the lipase, thereby giving access to the active site [29]. The catalytic site in lipases is structured by three α-amino acid residues located in the close vicinity of each other: serine, histidine, and aspartate or glutamate [27]. Lipase activation is facilitated by the attraction between the hydrophobic amino acids in the lid and the nonpolar side of the interface that lipase is adsorbing to [30]. Lipases from different sources exhibit the same type of lid conformational changes to open the active site: e.g., *Rhizomucor miehei* [30, 31], *Candida rugosa* [32], *Thermomyces (Humicola) lanuginosa* (TLL) [33, 34], *human pancreatic* (HPL) [35], *human gastric* (HGL) [36], and *dog gastric* (DGL) [37] lipases. The reactivity of catalytic proteins towards their substrates can be turned off by the presence of inhibitors, such as surfactants, bile salts, or fatty acid residues produced during the process of lipolysis [38]. It has been shown that bile salt micelles can also activate lipases inside an aqueous phase [39].

Lipases are different in their specificity. Some lipases are Sn-1,3 regiospecific, which means that they only remove the first and the third fatty acid side chains of triacylglycerols, such as gastric and pancreatic lipases. Thus, their hydrolysis of a triglyceride produces two fatty acids, or fatty acid salts, and one stable Sn-2 monoglyceride moiety [40]. On the other hand, some other lipases, like *Candida rugosa*, are non-regiospecific and can even cleave monoglycerides [27]. The selectivity of the lipase is also associated with a substantial role of the type of substrate that can become involved in enzymatic hydrolysis with the enzyme. A lipase can differentiate between enantiomers, and the relative sizes of the substituents at the stereocenter can determine the rate of the enzymatic reaction [41]. Inductive effect and steric hindrance are the two main elements in determining the rate of these reactions [42]. Among free fatty acids and mono-, di-, and triglycerides, Sn-1 monoglycerides are the most interfacially active products of the lipolysis and,

in competition with other species including lipase, can be adsorbed to the interface [43]. Extensive studies have been well investigated and documented elsewhere [25, 27, 43-46].

Interfacially adsorbed lipases may be either denatured due to a high interfacial tension or desorbed due to high interfacial pressure [47], both of which are functions of the surfactant concentration in the system. One of the prime interests for studying protein–surfactant interactions came from the detergent industry, where it was shown that these complexes can improve soil removal effects of detergents [48]. However, it has other striking applications in food industry [49], medicine [50], protein separation, and extraction [51-53]. Proteins and surfactants interact with each other through two main mechanisms: (i) electrostatic interaction between their charged groups—exclusive to ionic surfactants—and (ii) hydrophobic interaction between the nonpolar chain of the surfactant and lipophilic residues of the protein structure [54]. Thus, the type of surfactant charge plays a key role in this regard. Other environmental parameters that can affect protein–surfactant interactions are pH and ionic strength [27]; amino acids, the backbone of proteins, are amphoteric and can become cationic, zwitterionic, and anionic, from low to high pH values, respectively [55].

As mentioned above, categorizing lipase–surfactant interactions is not a straightforward task. The main findings about the interactions between different surfactants and lipases are summarized in *Table 1*. The source of the lipase is a crucial factor contributing to the interactions with surface-active agents. It is demonstrated that the kinetics of hydrolysis of *p*-nitrophenylbutyrate in presence of surfactants depends on the source of the lipase [56]. The isoelectric point, i.e., the pH at which a molecule is electrically neutral on average ($pH(I)$) [57], determines whether a protein is positively or negatively charged at each pH. On the surfactant side, several parameters play roles in their interaction with proteins. The chain-length of the cationic surfactants can increase their activation impact on the lipase [58]. In contrast, branched or linear chain ethoxylates have a completely different effect on the catalytic inhibition of *Rhizomucor miehei* [59]. The alkyl chain of the surfactant establishes the interaction with hydrophobic patches of the lipase molecules [60]. The surfactant monomers bind with their charged headgroups to the ionic amino acids of the protein: cationic surfactants to anionic groups (Glu, Asp) and anionic surfactants to cationic groups (Lys, Arg, His) [61]. Cationic surfactants exhibit a more profound interaction with lipase than other kinds of surfactants. For instance, *Rhizomucor miehei* has $pH(I)$ 3.5 [62], rendering it negatively charged in higher pH values and more attractive to positively charged surfactants. The interaction of cationic surfactants with lipases from different sources can lead to an activation [58, 63, 64], inhibition [64-66], or competitive adsorption at the interface [59, 63, 67, 68]. Also, the interaction of TTAB and *Thermomyces lanuginosus* lipase at pH 8 results in precipitation [64]. Inhibition [64, 69] and activation [64, 66] can be triggered by anionic surfactants. An amphoteric surfactant has revealed that only at low pH, i.e., in the cationic state, it interacts with lipase [62]. All kinds of surfactants can cause an activation followed by an inhibition, which means that, at low concentrations, monomers bring the lid to an open position, after which they accumulate at the active site and inhibit the substrate from effective binding [64]. Linear-chain ethoxylated nonionic surfactants are competitive inhibitors of lipase lipolysis, although the branched-chains exhibit no interaction or inhibition [59, 66].

Table 1- Lipase-Surfactant interactions, recent works, and achievements

Surfactant† (Type)‡	L§	Techniques	Main Findings	Ref
SDS (A)	PL	equilibrium dialysis,	• Bindings of SDS to lipase leads to fast and irreversible inactivation of enzyme; Under specific conditions, bile salts can prevent lipase inactivation by SDS;	[70]
SDS (A) TTAB (C)	HL	tensiometry, neutron reflectivity, NMR, microcalorimetry	• No interaction in bulk or at the interface; [SDS]* removes lipase from the interface; • Strong interaction at the water–air surface, but no distinct interaction in the bulk phase; At dilute concentrations, TTAB increases the lipase adsorption;	[67]
SHDDS (Am)	RM	tensiometry, ellipsometry,	• Surfactant–lipase binding only at cationic state; Lipase adsorption on top of the surfactant layer only at cationic state (cationic at *pH 3.0,* zwitterionic at *pH 7.5,* and anionic at *pH 10.5*);	[62]
DDAB (C)	RM	electrophoresis, Langmuir isotherm measurements, kinetic measurements	• Lipase binding to emulsion droplets stabilized by surfactant; Surfactant removes lipase from the droplet surface; Lipase adsorption to positively charged surfaces; High rate of reaction;	[63]
SBEHS (A)			• Lipase not binding to emulsion droplets stabilized by surfactant; Surfactant does not remove lipase from droplet surface; No lipase adsorption to negatively charged surfaces; No reaction	
EHEBHEGE (N)			• Inconclusive, since no change in droplet mobility; Either lipase interaction w/ surfactant or lipase impurity; High rate of reaction; Note: Different pH values were used to control the charge density of the adsorbed layers, *pH 4, 7.5, and 10*.	
SDS (A)	HL	Tensiometry, neutron reflectivity, ellipsometry,	• Lipase-surfactant complex formation neither in the bulk nor at the interface; No interaction between low [SDS] and adsorbed lipase layer; Protein displaced from the surface at high [SDS];	[68]
TTAB (C)			• Lipase–surfactant complex formation both in the bulk and at the interface; Thick lipase–surfactant layer at low [TTAB], removable by increasing surfactant concentration;	
SDS (A) CTAB (C) Brij-35 (N) CHAPS (Z)	RN	absorbance at 405 nm,	• 20% decrease in lipase activity • 30% decrease in lipase activity • 10% increase in lipase activity • 50% increase in lipase activity	[65]
LAS (A) Findet® 1214N/16, Findet®1214N/23, Glucopon® 650 (N)	TL	washing test,	• No inhibition of lipase activity (*pH 7*); • Decrease in lipase activity by prevention or delay in enzyme diffusion to the interface (*pH 8*);	[71]
AOT (A) DDDMAB (C)	RM	tensiometry, NMR, ellipsometry, electrophoresis,	• No lipase–surfactant complex formation; No inhibition for lipase; • Lipase–surfactant complex formation in bulk and at oil–water and solid–water interfaces;	[59]
β-OG (N), linear and branched ethoxylates (N)			• No lipase–surfactant complex formation; Competitive inhibition of linear-chain ethoxylates for lipase; No inhibition of branched-chain ethoxylates for lipase;	
SDS, SLE_2S (A)	TL	UV–vis spec., tensiometry, DLS, circular dichroism,	• Strong inhibition of lipase activity by SDS; Persevered structure and activity of lipase by SLE_2S (ethoxylated surfactant)	[69]
SDS, SOS (A) CTAB, TTAB, DTAB (C),	PA	double-beam spec.,	• Inhibition effect on lipase activity • Substantial improvement in lipase activity; Increase in activity by CTAB far above its CMC (0.8 mM); Chain-length correlation with activity improvement for cationic surfactants (CTAB>TTAB>DTAB);	[58]
Tween 80, Triton X-100 (N)			• Inhibition effect on lipase activity	
AOT (A) DDDMAB (C) Lin. C12EO4, Lin. C12EO5, Bra. C12EO8 (N)	Li RM	^{1}H-NMR, tensiometry,	• Fast palm oil hydrolysis with branched anionic surfactants; • Very slow palm oil hydrolysis with branched cationic surfactants; • Very slow palm oil hydrolysis with linear nonionic surfactants; Fast hydrolysis with branched nonionic surfactants;	[66]
SDS, SDSn (A) TTAB (C) OM, OG, DDM (N) lyso-MPG, lyso-MPC, lyso-LPC (Z),	TL	UVIKON 943 A spec., DLS, pyrene fluorescence,	• Lipase activation at low surf. conc. and lipase inhibition at high surf. conc. for all surfactants; • Activation to inhibition switch happening above CMC for anionic and cationic surfactants; Activation to inhibition switch happening far below CMC for nonionic and zwitterionic surfactants; • Monomeric surf. main responsible for the increase of activity;	[64]

†Surfactants: Sodium dodecyl sulfate (SDS) or sodium lauryl sulfate (SLS), tetradecyltrimethylammonium bromide (TTAB), sodium N-(2-hydroxydodecyl)sarcosinate (SHDDS), didodecyldimethylammonium bromide (DDAB), sodium bis(2-ethylhexyl)sulfosuccinate (SBEHS), 1-

(2-ethylhexyl)-3-(2-ethylbutyl)-2-hexaethylene glycerol ether (EHEBHEGE), linear alkylbenzene sulfonate (LAS); sodium bis(2-ethylhexyl)sulfosuccinate (AOT); didodecyldimethylammonium bromide (DDDMAB), β-1-octylglucoside (β-OG), sodium lauryl ether sulfate (SLE_2S), sodium octyl sulfate (SOS), dodecyltrimethylammonium bromide (DTAB), cetyltrimethylammonium bromide (CTAB), tetra(ethylene glycol) monododecyl ether (linear C12EO4), Penta(ethylene glycol) monododecyl ether (linear C12EO5), octa(ethylene glycol) mono(2-butyloctyl)ether (branched C12E08), sodium dodecyl sulfonate (SDSn), n-octyl-β-D-maltoside (OM), n-octyl-β-D-glucoside (OG), n-dodecyl-β-D-maltoside (DDM), 1-myristoyl-2-hydroxy-*sn*-glycero-3-phosphocholine (lyso-MPC), 1-myristoyl-2-hydroxy-sn-glycero-3-[phospho-rac-(1-glycerol)] (lyso-MPG), 1-lauroyl-2-hydroxy-*sn*-glycero-3-phosphocholine (lyso-LPC)

‡Surfactant types: anionic (A), cationic (C), nonionic (N), zwitterionic (Z), amphoteric (Am)

§Lipase (L): pancreatic lipase (PL), Humicola lanuginose (HL), Rhizomucor miehei (RM), Rhizopus niveus (RN), Thermomyces lanuginosus (TL), Pachira aquatica (PA), Lipozyme (Li)

*Square brackets denote concentration.

Note: All of the studies in the table have been conducted in phosphate-buffered saline solution or pure water solution of pH between 7 to 8, unless otherwise stated.

Even after more than three decades of intense investigations, several aspects of lipase–surfactant interactions are still not well understood. The present work studies the dynamic competitive adsorption of lipase (from *Candida rugosa*) and ionic surfactants (SDS and CTAB) at the water–air interface. For this purpose, a coaxial double-capillary combined with a drop profile analysis tensiometer is used, which allows parallel measurements of the dynamic surface tension and interfacial elasticity of single and mixed layers. By employing different injection–suction protocols, we are able to study the adsorption and desorption inside the lipase–surfactants system in detail, and to conclude onto the different interactions between lipase and generic ionic surfactants. Reversibility of the adsorption process, the effect of anionic and cationic surfactants on the adsorption of lipase, the likelihood of lipase–surfactant complex formation at the interface, and the importance of the interfacial elasticity values for studying lipase–surfactant complexes are discussed this work.

2 Materials and Methods

2.1 Chemicals

Candida rugosa lipase with trade name *Lipomod™ 34P-L034P* was purchased form *Biocatalysts Ltd* (*Cardiff, UK*) and used without further purification. *Cetyltrimethylammonium bromide* (CTAB, *purity ≥ 98% by TLC*) and *sodium dodecyl sulfate* (SDS, *Ph Eur Grade*) were purchased from *Merck* (*Darmstadt, Germany*). All of the solutions were prepared at room temperature (*22 °C*) using phosphate-buffered saline (*Sigma-Aldrich*) with pH *7.2–7.4* and ionic strength of *0.17 M*.

2.2 Coaxial Double Capillary Profile Analysis Tensiometry

To explore the sequential adsorption of surfactant and lipase to the same liquid–fluid interface, we have utilized the profile analysis tensiometer *PAT1* (*SINTERFACE Technologies, Berlin, Germany*), equipped with a coaxial double capillary providing drop exchange processes via an injection–suction protocol with an accuracy of *0.1 mm³* (*Figure 1* Figure 2). The methodolgy has been introduced in [72-77], and the experimental protocol and efficient flow exchange conditions have been investigated recently in [78, 79]. The double-dosing syringe configuration connected to the double capillary enables us to exchange the internal phase of a droplet without interrupting the interfacial layer [78]. To achieve this aim, the secondary phase can be injected from the inner capillary to displace the primary bulk phase of the droplet and sweep it out via the outer capillary. The droplet profile is fitted to the *Young-Laplace* equation [80, 81] to gain the interfacial properties of the system. This powerful tool allows us to investigate the effect of sequential adsorption/desorption of surfactant, protein, polymer, nanoparticle, etc., and their related complexes.

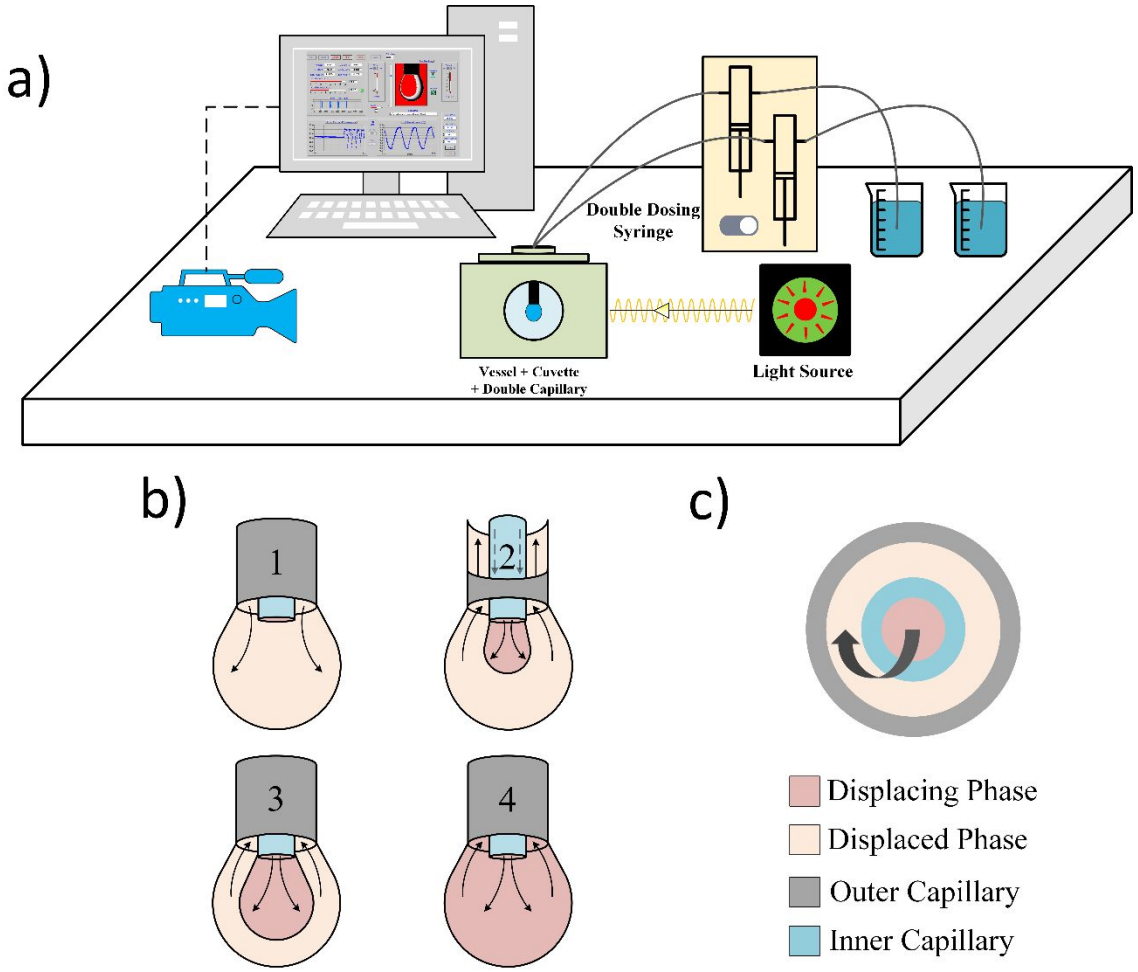

Figure 1- (a) Schematic experimental setup of a PAT with s coaxial double capillary , (b) side view of the double capillary with a drop formed at its tip and the flow exchange pattern; the secondary phase is injected from the inner capillary into the droplet, displaces the primary phase through the outer capillary via a combined suction flow; (c) cross-section view of the double capillary system and the liquid pathway

2.3 Interfacial Rheology

Different surface-active agents, besides their effect on interfacial tension (IFT), can form various interfacial structures and textures. The interfacial dilational rheology of adsorbed layers can be investigated using the same methodology, however, based on protocols that generate harmonic compressions and expansions of the interfacial area. During the generated harmonic perturbations, the interfacial tension variations as the response of the adsorbed layers are recorded. For sinusoidal perturbations, the amplitude and phase shift of the IFT variations are measured for the dilational elasticity and viscosity of the interfacial layer, respectively [82]. The visco-elasticity of an interfacial layer can be formulated in a complex domain as [83, 84]:

$$E(i\omega) = E' + E''i = E_0 \frac{\sqrt{i\omega}}{\sqrt{i\omega} + \sqrt{2\omega_0}} \quad (1)$$

$$E' = E_0 \frac{1 + \sqrt{\omega_0/\omega}}{1 + 2\sqrt{\omega_0/\omega} + 2\omega_0/\omega} \quad (2)$$

$$E'' = E_0 \frac{\sqrt{\omega_0/\omega}}{1 + 2\sqrt{\omega_0/\omega} + 2\omega_0/\omega} \quad (3)$$

$$\omega_0 = \left[\frac{dC}{d\Gamma}\right]^2 \left(\frac{D}{2}\right) \quad (4)$$

$$E_0 = -\frac{d\gamma}{dln\Gamma} \quad (5)$$

where E, E' and E'' are the complex visco-elasticity and its real and imaginary components ($mN.m^{-1}$), E_0 is the elasticity modulus (high-frequency limit), ω is the circular frequency, C is the bulk concentration, Γ is the interfacial excess concentration ($mol.m^{-2}$), D is the diffusion coefficient, and ω_0 is the characteristic frequency, defined on the basis of the properties of the surface-active molecule. In this way, the two parameters, interfacial elasticity $|E|$ and phase angle ϕ, are defined which characterize the complex viscoelastic behavior:

$$|E| = \frac{E_0}{1 + 2\sqrt{\omega_0/\omega} + 2\omega_0/\omega} \quad (6)$$

$$\phi = \tan^{-1}\left(\frac{\sqrt{\omega_0/\omega}}{1 + \sqrt{\omega_0/\omega}}\right) \quad (7)$$

This formulation is easily applicable when the adsorption model provides an analytical function between bulk concentration and interfacial excess concentration [85]. In harmonic perturbations, usually a sinusoidal change of the drop volume and hence of the drop area is made [86]:

$$A(t) = A_0 + \Delta A \times \sin(\omega t + \phi_A) \quad (8)$$

where A is the areal perturbation, A_0 is initial or mean area of the droplet, and ΔA,ω and ϕ_A are the amplitude, angular frequency, and phase angle of the sinusoidal perturbation. In response, the interfacial tension oscillates in the following manner:

$$\gamma(t) = \gamma_0 + \Delta\gamma \times \sin(\omega t + \phi_\gamma) \quad (9)$$

The elasticity and viscosity of the interfacial area can be calculated as follows:

$$E = \frac{d\gamma}{dlnA} \cong A_0 \frac{\Delta\gamma}{\Delta A} \quad (10)$$

$$\phi = \phi_\gamma - \phi_A \quad (11)$$

2.4 Experimental Protocol and Elasticity Measurement

To conduct an experimental analysis using the coaxial double capillary setup, an experimental protocol has been introduced to change the bulk phase of a pendant droplet to inspect the influence of sequential adsorption of surface-active agents onto the same interface [72, 73, 87]. We have used this methodology to explore the dynamics of adsorption/desorption of lipase, SDS, and CTAB at the water–air interface considering different experimental protocols including non-competitive/competitive, and sequential/simultaneous cases. The schematic of the experimental protocol is shown in *Figure 2*, demonstrating how the injection of a new phase affects the interfacial response of the droplet. As an example, let us consider the following case: a lipase solution droplet is formed as the primary phase. The lipase adsorbs at the interface and forms an interfacial layer. Then, a solution of the first surfactant (S1)

displaces the bulk of the droplet to study the competitive adsorption of lipase and S1. After that, a fresh solution of a second surfactant (S2) is injected into the droplet to remove the S1 solution and to study the competitive adsorption of lipase, S1, and S2. Finally, a buffer solution is injected to sweep away the S2 solution and study the desorption of lipase, S1, and S2. During the injection of different solutions, the interfacial tension usually decreases, owing to the co-adsorption of surface-active agents.

To explore the visco-elasticity of the interfacial layers, harmonic oscillations are imposed on the interfacial area of the droplet with a specified amplitude and frequency over a certain time interval Δt. From the IFT response, the visco-elasticity of the adsorbed layer can be determined. The larger the amplitude of the IFT response, the higher is the measured elasticity of the adsorbed layer. The Fourier Transform application of the PAT software was used to calculate the elasticities via sinusoidal function fittings for $A(t)$ and $\gamma(t)$ according to *Eq. 8–10*.

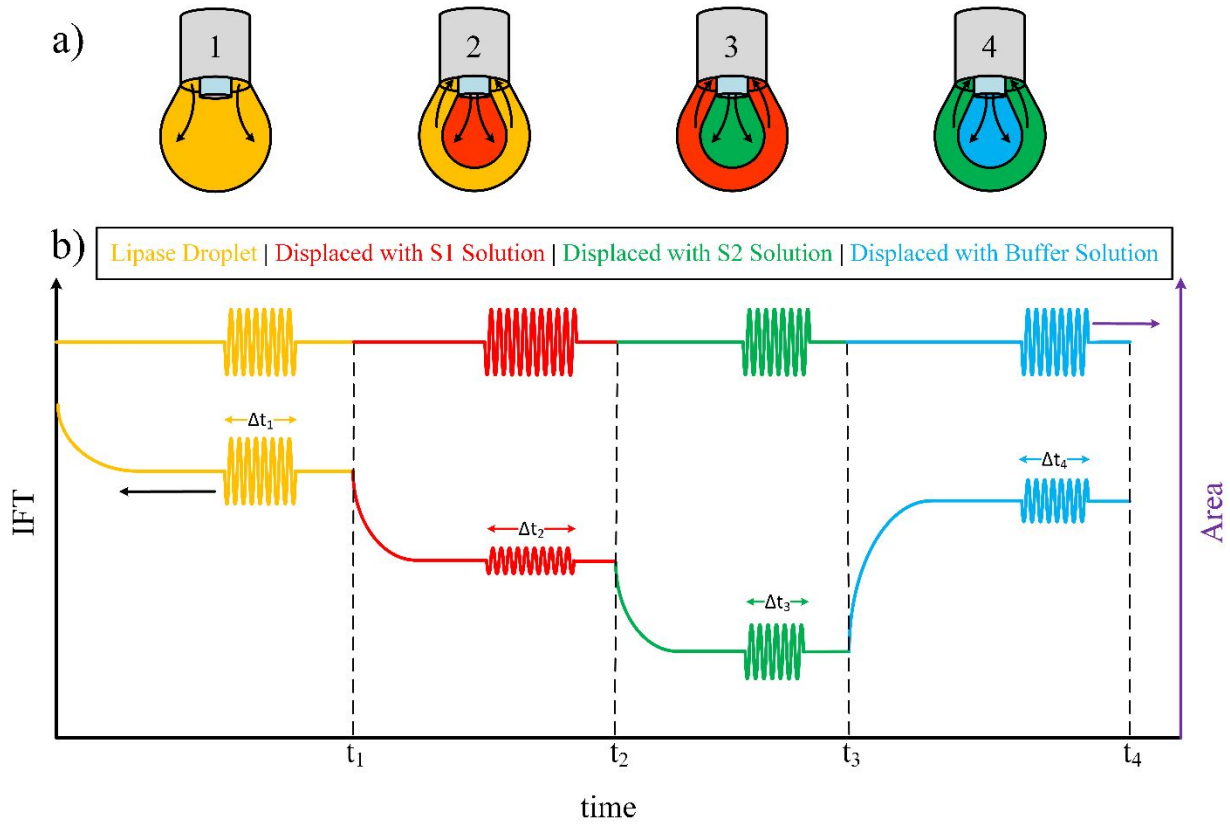

Figure 2- Schematic representation of the experimental protocol for exchanging the bulk phase of a droplet while the interface remains intact. a) (1) the primary phase (e.g., lipase solution) is injected from the external capillary to form a drop at which the primary interfacial layer is formed; (2) the primary phase is displaced with the secondary phase (e.g., S1 solution) after t_1, injected from the internal capillary; (3) the secondary phase is displaced with the tertiary phase (e.g., S2 solution) after t_2, injected from the internal capillary; (4) the tertiary phase is displaced with the quaternary phase (e.g., buffer solution) after t_3, injected from the internal capillary; b) The interfacial area of the droplet is controlled during the test to remain constant except for harmonic oscillations with the specified frequency and amplitude imposed on the interfacial area of the droplet for Δt seconds to investigate the interfacial rheology; IFT responses to the concentration changes caused by the harmonic area oscillations for the mentioned systems are shown in different colors; the values of IFT determine the levels of competitive adsorption or desorption, and the

amplitudes of IFT sinusoidal oscillations determine the elasticity of the adsorbed layer and its structure formation.

3 Results

3.1 Adsorption and Desorption of SDS, CTAB, and Lipase

The adsorption and desorption of SDS, an anionic surfactant with a CMC of about *8.2 mM* in pure water [88], at the water–air interface was studied by sequential injection of SDS and buffer solutions inside a pendant drop (

Figure 3 *a)*. In the first test (⋄), a buffer solution droplet formed in air is exchanged with an SDS solution, *2.0 mM*. So, the interfacial tension (IFT) is quickly reduced to around *44 mN.m*$^{-1}$ due to the given concentration of SDS in the bulk, causing a fast diffusion process supported by the convection inside the droplet. After that, the exchange process was continued with the buffer solution to remove the SDS solution from the drop. A rapid increase in surface tension is observed approaching the initial value for the buffer solution. These results indicate that an efficient bulk exchange leads to a complete SDS desorption from the interface, which demonstrates the reversible adsorption of this classic surfactant. In another test (○), first, a *2 mM* SDS solution drop was formed, the SDS molecules adsorbed at the interface, reaching an equilibrium (within about *300 s*) with an IFT identical with the value of the previous test (around *44 mN.m*$^{-1}$). Then, the first set of surface dilational elasticity measurements was performed ($t = 600–700\ s$). Afterwards buffer solution was injected into the droplet to drain the bulk concentration of the SDS solution abruptly, which increased the IFT again to the same level of the buffer solution. The second set of elasticity measurements was performed at $t = 1300–1400\ s$. The two experiments show that, regardless of being the primary or secondary phase inside the droplet, SDS can be completely washed away from the interface. Moreover, the given results demonstrate the efficiency of our drop protocol to an exchange of its bulk by 100%. This protocol was applied to CTAB and lipase solutions in an equivalent way.

In

Figure 3 *(a)* (▵) the results of the Lipase adsorption during drop bulk exchange are presented. The lipase solution of *2.5 mg.mL*$^{-1}$ has a surface tension of about *50 mN.m*$^{-1}$ and the system approaches the equilibrium value after about *500 s*. The first set of visco-elasticity measurements was performed at $t = 600–700\ s$ and then buffer solution was injected into the droplet to exchange the bulk. However, the IFT did not show any significant changes during the sub-phase exchange, because the lipase molecules did not desorb from the interface. Unlike the surfactants, the adsorption free energy per particle is large for proteins, making the desorption process energy-intensive. This irreversible adsorption behavior can also be explained by the hydrophobic residues of the lipase molecules. These residues have been buried inside the protein while solved in the aqueous phase and change their conformation once exposed to the nonpolar air phase. So, the interfacial evolution makes the lipase unfold and hence unable to leave the interface. Thereby the IFT remains approximately the same despite the displacement of lipase solution by the buffer solution inside the drop. The second set of the elasticity measurements at $t = 1300–1400\ s$ supports this finding. It shows elasticity values even higher than those observed before the bulk exchange, since the non-adsorbed lipase molecules have been washed away during buffer solution exchange, and no lipase is left to be adsorbed during the interfacial area expansion. The slightly increased elasticity can also be explained by slow structure changes in the interfacial lipase layer.

The results of the CTAB exchange with buffer solution are shown in

Figure 3 *(b)*. CTAB is a cationic surfactant with a CMC of about *0.9 mM* in pure water at *25 °C* [89], one order of magnitude less than SDS. For this CTAB solution, the IFT decreases to around *52 mN.m*$^{-1}$ (+). Then, this solution was exchanged with buffer solution and the IFT returned to its initial value for a pure

buffer solution. This means CTAB desorbs from the water–air interface completely by washing out with the buffer solution. In the second test (▫), a buffer droplet was exchanged with the same CTAB solution, which then was replaced again by the buffer solution. During CTAB injection, the IFT decreased even beyond the quasi-equilibrium value observed in the previous experiment. This phenomenon can be explained by the quick adsorption during a convective bulk exchange with the CTAB solution.

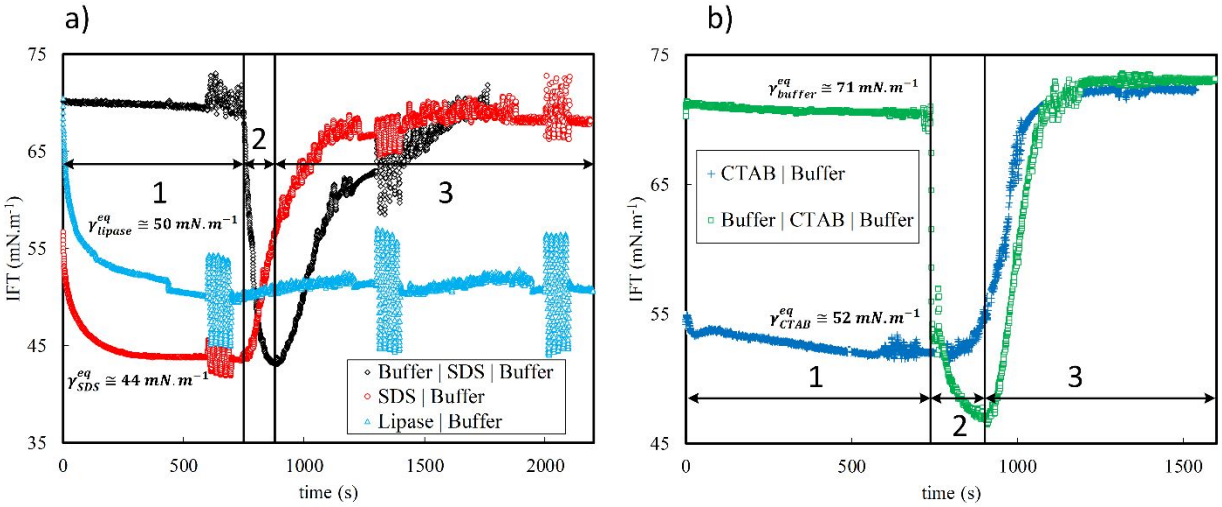

Figure 3- Dynamic interfacial tension for SDS, CTAB, and lipase at water–air interfaces during different experiments of drop bulk exchange: a) (◇) buffer droplet in air (1), displaced by 2.0 mM SDS solution (2) and then again by the buffer solution (3); (○) 2.0 mM SDS solution (1), displaced by the buffer solution (2&3); (△) 2.5 mg.mL^{-1} lipase solution (1), displaced by the buffer solution (2&3); b) (▫) buffer solution droplet (1), displaced by 0.5 mM CTAB solution (2) and then by the buffer solution (3); (+) 0.5 mM CTAB solution (1), displaced by the buffer solution (2&3). The first exchanges occurred after 715 seconds from the start of the test.

3.2 Competitive Adsorption and Desorption of SDS and Lipase

Studies on the competitive adsorption and desorption of SDS and lipase at the water–air interface can provide us a better insight into their interaction in the bulk and at the interface. The results for simultaneous and sequential adsorption and desorption are summarized in *Figure 4*. In the first test (◇), the primary lipase solution in the drop was displaced by a SDS solution and then by the buffer solution. In the second test (○) , the primary SDS solution was displaced by a lipase solution and then by the buffer solution. In the third test (△), a drop of a premixed SDS & lipase solution was studied as the primary phase and then displaced by a buffer phase. The IFT reduces from about *50 mN.m^{-1}* (lipase solution as the primary phase), via *~39 mN.m^{-1}* (SDS) to about *31 mN.m^{-1}* for the mixed SDS and lipase solution. This basic information indicates that SDS and lipase can simultaneously adsorb at the water–air interface and decrease the IFT to values lower than those for the single-component solutions. The elasticity values from *Figure 4 (b),* corresponding to the moment before the drop bulk exchange process ($t = 600–700\ s$), show a similar behavior like the IFT. The maximum value *30.9 mN.m^{-1}*, attained for the adsorbed layer of lipase, decreases via *12.4 mN.m^{-1}* (SDS) towards *8.0 mN.m^{-1}* for the premixed SDS–lipase layer. The higher elasticity for the SDS layer compared to the SDS–lipase layer can be attributed to dodecanol, always present to a unknown extent in SDS samples [90].

The results of the injection of a secondary phase and drop sub-phase exchange in *Figure 4* deliver additional information about the adsorption layer composition and the interactions in the bulk and at the interface. Displacing the lipase solution in the droplet by the SDS solution results in a quick reduction of IFT to values lower than those for pure SDS but higher than those for the SDS–lipase mixed adsorption layer. For a certain time (about 100 s) during the exchange, we see a low IFT implying that SDS adsorbs at the available

places at the interface in competition with the lipase. Afterwards, we observe a quick increase in IFT which is mainly due to the decrease of the SDS concentration due to the exchange process which is followed by the buffer solution exchange after the SDS solution. The 2nd set of elasticity measurements in *Figure 4 (b)* ($t = 1300–1400\ s$) shows that the elasticity values for different displacing scenarios are between those of pure SDS and pure lipase layers ($t = 600–700\ s$) based on the amplitude of the IFT curves. This indicates the presence of a mixed SDS–lipase adsorption layer. With the continuation of the sub-phase exchange with buffer solution after *1400 s*, we see an increase in the IFT, approaching values similar to those for a pure lipase layer. However, the 3rd elasticity measurements at around $t = 2000–2100\ s$, leads to values much lower than those for the single lipase layer, suggesting still the presence of a mixed SDS–lipase layer even after the exchange with the buffer solution. We can compare it with the exchange of an SDS drop with the buffer solution, showing complete desorption of SDS from the water–air interface. Therefore, we conclude a weak interaction between SDS and lipase, as SDS cannot be completely removed via an exchange with buffer solution. However, the adsorbed layer is not in a complex structure behaving like a highly elastic layer. We discuss this situation further below in terms of the surface charge distribution.

An SDS layer displaced by lipase shows certain similarities with the case of SDS displacing a lipase layer. However, the former case leads to a lower IFT similar to the pre-mixed SDS–lipase layer (simultaneous adsorption protocol), followed by a much faster increase in IFT because of the faster desorption of SDS during the exchange process. The elasticity after the 1st and 2nd drop bulk exchange processes shows almost similar values, indicating similar mixed SDS–lipase layers for both systems. However, the elasticity value for an SDS solution displaced by a lipase solution is about *20.7 mN.m^{-1}*, which is slightly higher than for the lipase layer displaced by SDS, for which we found elasticity values of about 16.3 mN.m^{-1}.

In summary, these results indicate that SDS and lipase can be co-adsorbed in competitive adsorption according to their concentration and injection time, and SDS can desorb from the interface when the SDS concentration in the bulk is decreased. However, lipase decreases the rate of SDS desorption, and adsorbed lipase cannot be significantly removed from the interface even in the presence of SDS at the given conditions (pH and ionic strength).

The mixed SDS–lipase pre-adsorbed layer after the bulk exchange with buffer solution shows a different behavior. The large elasticity values after one exchange process explain that SDS is removed from the interface while lipase remains. This underlines that lipase can adsorb in the presence of SDS very well provided that there is enough time and a sufficiently high concentration in the bulk. Also, the adsorbed SDS molecules among the lipase molecules can be still removed from the interface. These results are in line with those obtained for the other two cases discussed in *Figure 4*, namely SDS exchanged by lipase, and vice versa.

3.3 Competitive Adsorption and Desorption of CTAB and Lipase

Competitive sequential adsorption and desorption experiments of CTAB and lipase are presented in *Figure 5.* There is a different behavior observed when compared with the SDS–lipase system presented in *Figure 4*. First, when lipase is displaced from the surface by a CTAB solution (○), the IFT substantially and quickly decreases, which is similar to the exchange of a lipase layer by SDS. However, exchanging the CTAB solution now by the buffer solution results in just a slight increase in IFT, while exchanging the SDS solution by buffer solution shows a significant IFT increase. These results indicate that after removing CTAB from the bulk, the adsorbed CTAB molecules inside the lipase layer do not desorb easily, revealing a stronger lipase–CTAB interaction compared to lipase–SDS. The decreasing elasticities from *31.3 mN.m^{-1}* ($t = 600–700\ s$) for the lipase layer to *9.3 mN.m^{-1}* after exchange with CTAB ($t = 1300–1400\ s$) also support

that CTAB remains inside the lipase layer, causing a significant decrease in elasticity. These values are close to the elasticity of a single CTAB adsorbed layer, which is about *6.1 mN.m*$^{-1}$ ($t = 600–700\ s$).

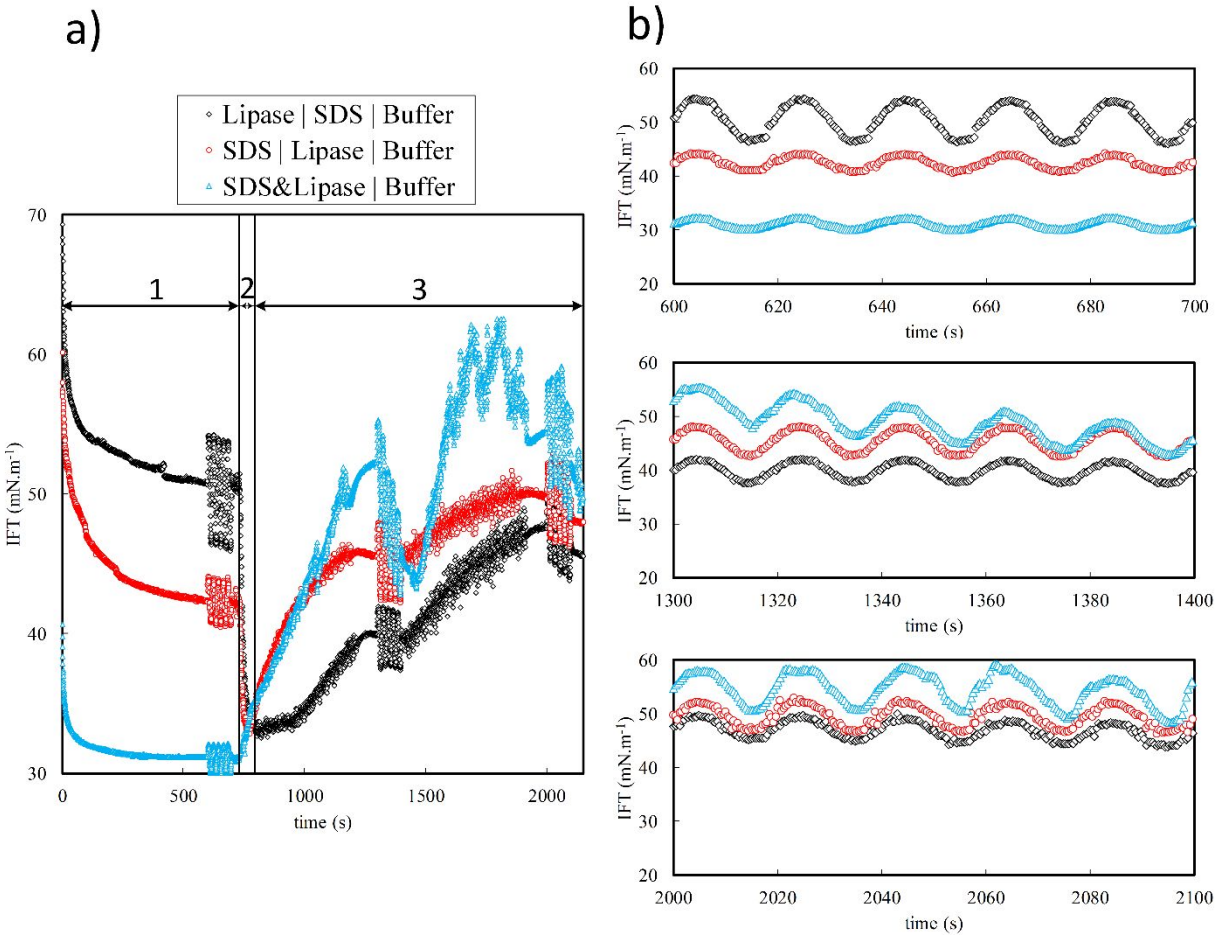

Figure 4- Interfacial tension (IFT) during dynamic competitive adsorption of SDS and lipase, sequential and simultaneous drop bulk exchange protocols at the water–air interface: a) (◇) 2.5 mg.mL^{-1} *lipase solution (1), displaced by 2.0 mM SDS solution (2) and then by the buffer solution (3); (○) 2.0 mM SDS solution (1), displaced by 2.5 mg.mL*$^{-1}$ *lipase solution (2) and then by buffer solution (3); (△) 2.5 mg.mL*$^{-1}$ *lipase premixed with 2.0 mM SDS solution (1), displaced by the buffer solution (2&3); b) IFT of the same solutions in response to the droplet volume harmonic oscillations with 0.05 Hz frequency and 2 mm*^{3} *amplitude, introduced between 600–700, 1300–1400, and 2000–2100 seconds.*

The results for the CTAB bulk exchanged with lipase shown in *Figure 5* provide us additional information about the CTAB–lipase interaction. They illustrate a fast decrease in IFT at the beginning of the exchange (about $t = 700\ s$), i.e., a fast co-adsorption of lipase inside the pre-adsorbed CTAB layer. However, in continuation of the exchange, the surface tension subsequently increases due to the removal of CTAB from the bulk and consequently the desorption of CTAB from the surface. This demonstrates that lipase adsorption can remove a certain part of CTAB from the interface, and still gradual adsorption of lipase is going on. The large elasticity value after the exchange (*26.5 mN.m*$^{-1}$ for $t = 1300–1400\ s$) demonstrates that lipase is the major adsorbed component at the interface after a partial CTAB substitution. Besides, as the IFT values are lower than those for the pure lipase layer, it shows the existence of CTAB molecules inside the adsorbed layer. According to the large elasticity values, we can conclude that lipase–CTAB mixed

layers can contain stable complexes, in contrast to the mixed lipase–SDS layers for which smaller elasticities were observed.

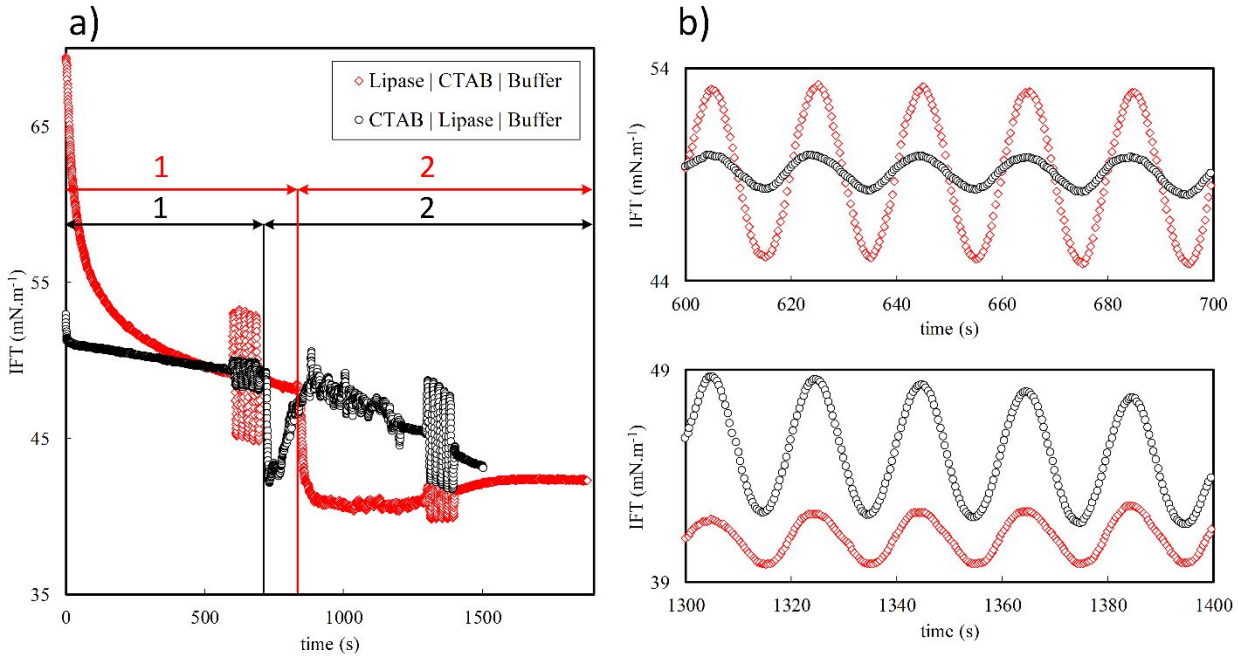

Figure 5- Interfacial tension during the dynamic competitive adsorption of CTAB and lipase generated by a sequential exchange protocol: a) (◇) 0.5 mM CTAB solution (1), displaced by a lipase solution and then by buffer solution (2); (○) 2.5 mg.mL^{-1} lipase solution (1), displaced by 0.5 mM CTAB solution and then by buffer solution (2); b) IFT of the same solutions in response to harmonic oscillations of the droplet volume with a frequency of 0.05 Hz and amplitude of 2 mm^3, generated between 600–700 and 1300–1400 seconds, respectively.

3.4 Competitive Adsorption of Lipase SDS, and CTAB: Sequential and Mixed Protocols

For a better understanding of the dynamic competitive adsorption of lipase, SDS and CTAB and the related interactions in the bulk and at the interface, exchanges of pre-adsorbed lipase layers (*2.5 mg.mL^{-1}*) with SDS (*2.0 mM*) and CTAB (*0.5 mM*) in sequential and simultaneous scenarios were performed. For the sequential protocol, i.e., lipase|CTAB|SDS|buffer and lipase|SDS|CTAB|buffer sequences, we observe a sharp and significant decrease in IFT. In the simultaneous injection of SDS and CTAB, the decrease in IFT is not as profound as their sequential injection. Note, all CTAB cations are compensated by the same number of SDS anions forming ion pairs and only the remaining amount of SDS ions is available for the interaction with the lipase. These results demonstrate the importance of the electrostatic interactions of CTAB and lipase, missed in the case of exchange by a mixed SDS–CTAB solution. The nonionic SDS–CTAB ion pairs [90] can be co-adsorbed into the lipase layer, although via rather hydrophobic interactions. The elasticities also support these findings, as we see the lowest elasticity for the case of mixed SDS–CTAB solution because there is no opportunity for lipase–CTAB complex formation. The highest elasticity belongs to the CTAB|SDS|buffer scenario, which is also in correlation with the hypothesis that the pre-adsorbed lipase can keep the attached CTAB molecules during the first exchange. During removal of CTAB from the bulk by SDS injection, lipase–CTAB complexes can remain and exhibit high elasticity values.

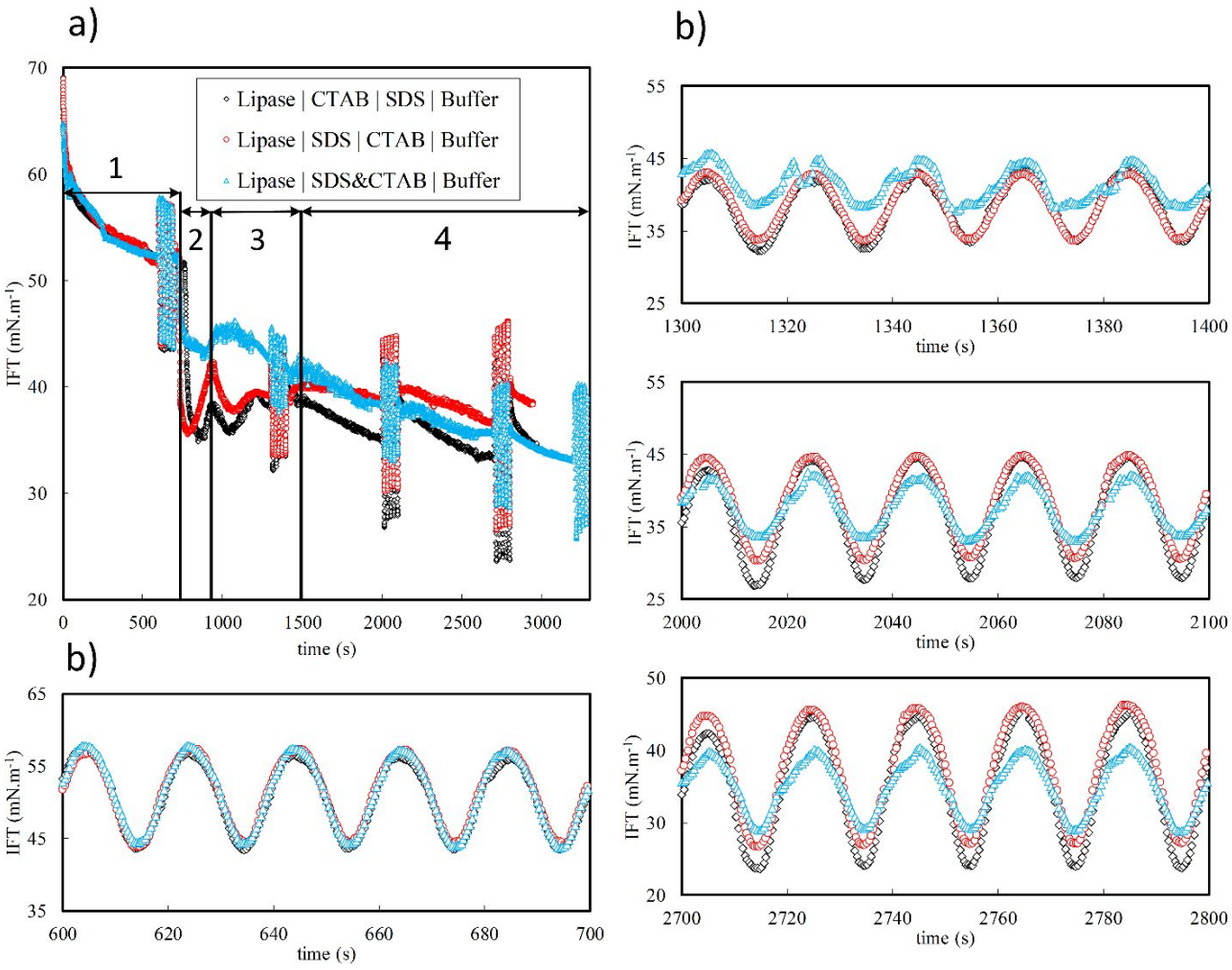

Figure 6- Dynamic competitive adsorption of lipase, SDS, and CTAB at the water–air interface via sequential and simultaneous SDS and CTAB exchange protocols. Interfacial tension vs. time of a) (◇)2.5 mg.mL^{-1} lipase solution (1), displaced by 0.5 mM CTAB solution (2) then by 2.0 mM SDS solution (3), and finally by a buffer solution (4); (○) 2.5 mg.mL^{-1} lipase solution (1), displaced by 2.0 mM SDS solution (2), then by 0.5 mM CTAB solution (3), and finally by a buffer solution (4); (△) 2.5 mg.mL^{-1} lipase solution (1), displaced by a mixed CTAB–SDS (0.5 mM and 2.0 mM) solution (2), and then by a buffer solution (3&4); b) IFT of the same solutions in response to the droplet volume harmonic oscillations at a frequency of 0.05 Hz and amplitude of 2 mm^3, generated between 600–700, 1300–1400, 2000–2100, and 2700–2800 seconds.

4 Molecular Structural Analysis

A molecular structure analysis was performed via the PyMOL molecular visualization system which is based on a Poisson–Boltzmann equations solver (created by Warren, Lyford, and DeLano) [91] for exploring surface charges of *Candida rugosa* lipase to gain a better insight into the results observed by dynamic surface tension measurements and competitive adsorption analysis. The electrostatic potential map projected on the molecular surface of the lipase molecule presented in *Figure 7* shows a dominant negatively charged surface, which is in correlation with the stronger attachment of the cationic surfactant CTAB presented in *Figure 4–Figure* 6. We can also see minor positive regions that can support a partial

attraction of SDS to the lipase surface via electrostatic interactions. However, at the water-air surface, SDS is adsorbed rather via a competitive adsorption mechanism, forming a mixed adsorbed layer with the lipase molecules, while CTAB can adsorb in the form of complexes with lipase. Such computational simulations and the macromolecular structure analysis to explore the surface charges of the lipase lay the basis for an understanding of the probable molecular interactions (e.g., with surfactants). However, complementary experimental techniques such as dynamic surface tension measurements, dilational surface visco-elasticity, and competitive adsorption analysis help understanding the concrete realization of these interactions. It is noted that changing pH, temperature, and presence of salts and ions can change the surface charges and affect these observed interactions significantly.

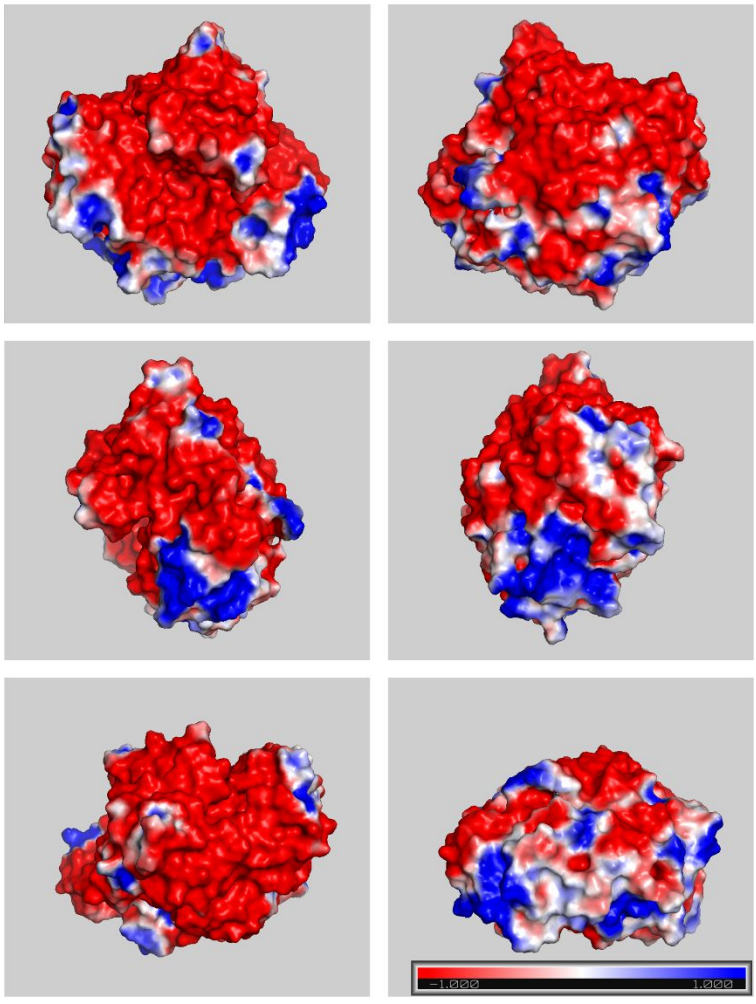

Figure 7- Projection of the electrostatic potential of a Candida rugosa lipase (PDB ID: 1LPN [32]) on its molecular surface from six different angles (front, back, left, right, top, and bottom). The electrostatic potential of +1 and more is blue and that of -1 and less is red. Illustrated using PyMOL Version 2.3.5 [91].

5 Conclusions

Our results demonstrate that dynamic surface tension measurements and interfacial rheology characterizations using PAT tensiometer equipped with a co-axial double capillary for drop sub-phase exchange, can provide us insightful data about the dynamic competitive adsorption of mixed lipase-surfactant layers and complex formation in the bulk and at the interface. Our results can be summarized as follows: I- For a pre-adsorbed layer of SDS or CTAB, when the bulk is displaced with a buffer solution, SDS and CTAB completely desorb from the interface, illustrating a reversible adsorption process. II- A pre-adsorbed lipase layer cannot be removed via the sub-phase exchange process by a buffer solution (pH 7.2–7.4). III- The sub-phase exchange by SDS and CTAB solutions also cannot remove the pre-adsorbed lipase. SDS can participate in the formation of mixed adsorption layers with lipase via competitive adsorption at the available positions, while CTAB can form complexes in the bulk and at the interface, which is supported by the observed higher dilational elasticity. Lipase can cause significant entrapment of CTAB in the mixed layer as a joint adsorbed complex via electrostatic interactions between oppositely charged sites. However, SDS is also entrapped inside the lipase layer via hydrophobic interactions and partial electrostatic interactions. The explored surface charges of the lipase via computational structure analysis corroborates these conclusions, considering expected strong electrostatic interactions with the cationic CTAB rather than the anionic SDS.

Understanding of the interactions of the lipase with surfactants and assessment of the related dynamic competitive adsorption at the interface via the presented experimental protocols are essential for the optimization of multicomponent multiphase processes involved in reactive interfacial phenomena. Such processes can influence significantly the phase distribution and interfacial area and consequently the interfacial transport properties and kinetics of the conversions. Further experiments and analysis under different conditions (pH, T, concentration, ionic strength, flow exchange conditions, and sequence of substances) are needed to conclude on the expected interactions in the bulk and competitions at the interface for the design of other multiphase processes and their optimization.

6 Acknowledgment

Funded by the German Research Foundation (DFG) - TRR 63 "Integrated Chemical Processes in Liquid Multiphase Systems" (subproject Z1) – 56091768 (Gefördert durch die Deutsche Forschungsgemeinschaft (DFG) - TRR 63 "Integrierte chemische Prozesse in flüssigen Mehrphasensystemen" (Teilprojekt Z1) – 56091768). We would like also to appreciate the financial support provided by the Dresden Excellence Fellowship of TU Dresden.

7 References

[1] A. Svendsen, Lipase protein engineering, Biochimica et Biophysica Acta (BBA) - Protein Structure and Molecular Enzymology 1543(2) (2000) 223-238.
[2] F. Luddy, R. Barford, S. Herb, P. Magidman, R. Riemenschneider, Pancreatic lipase hydrolysis of triglycerides by a semimicro technique, Journal of the American Oil Chemists' Society 41(10) (1964) 693-696.
[3] H.L. Brockman, W.E. Momsen, T. Tsujita, Lipid-lipid complexes: Properties and effects on lipase binding to surfaces, Journal of the American Oil Chemists' Society 65(6) (1988) 891-896.
[4] A. Fröhlich, B. Rice, G. Vicente, The conversion of low grade tallow into biodiesel-grade methyl ester, Journal of the American Oil Chemists' Society 87(7) (2010) 825-833.
[5] I.B. Banković-Ilić, I.J. Stojković, O.S. Stamenković, V.B. Veljkovic, Y.-T. Hung, Waste animal fats as feedstocks for biodiesel production, Renewable and sustainable energy reviews 32 (2014) 238-254.

[6] A. Demirbas, S. Karslioglu, Biodiesel production facilities from vegetable oils and animal fats, Energy Sources, Part A 29(2) (2007) 133-141.
[7] F. Ma, L.D. Clements, M.A. Hanna, Biodiesel fuel from animal fat. Ancillary studies on transesterification of beef tallow, Industrial & engineering chemistry research 37(9) (1998) 3768-3771.
[8] R. Altın, S. Çetinkaya, H.S. Yücesu, The potential of using vegetable oil fuels as fuel for diesel engines, Energy Conversion and Management 42(5) (2001) 529-538.
[9] S. Clark, L. Wagner, M. Schrock, P. Piennaar, Methyl and ethyl soybean esters as renewable fuels for diesel engines, Journal of the American Oil Chemists' Society 61(10) (1984) 1632-1638.
[10] M. Mittelbach, P. Tritthart, H. Junek, Diesel fuel derived from vegetable oils, II: emission tests using rape oil methyl ester, Energy in Agriculture 4 (1985) 207-215.
[11] M. Mittelbach, P. Tritthart, Diesel fuel derived from vegetable oils, III. Emission tests using methyl esters of used frying oil, Journal of the American Oil Chemists' Society 65(7) (1988) 1185-1187.
[12] P.R. Muniyappa, S.C. Brammer, H. Noureddini, Improved conversion of plant oils and animal fats into biodiesel and co-product, Bioresource technology 56(1) (1996) 19-24.
[13] B. Supple, R. Howard-Hildige, E. Gonzalez-Gomez, J. Leahy, The effect of steam treating waste cooking oil on the yield of methyl ester, Journal of the American Oil Chemists' Society 79(2) (2002) 175-178.
[14] M. Hajjari, M. Tabatabaei, M. Aghbashlo, H. Ghanavati, A review on the prospects of sustainable biodiesel production: A global scenario with an emphasis on waste-oil biodiesel utilization, Renewable and Sustainable Energy Reviews 72 (2017) 445-464.
[15] S. Zheng, M. Kates, M. Dubé, D. McLean, Acid-catalyzed production of biodiesel from waste frying oil, Biomass and bioenergy 30(3) (2006) 267-272.
[16] Y. Watanabe, Y. Shimada, A. Sugihara, Y. Tominaga, Enzymatic conversion of waste edible oil to biodiesel fuel in a fixed-bed bioreactor, Journal of the American Oil Chemists' Society 78(7) (2001) 703-707.
[17] B.-X. Peng, Q. Shu, J.-F. Wang, G.-R. Wang, D.-Z. Wang, M.-H. Han, Biodiesel production from waste oil feedstocks by solid acid catalysis, Process Safety and Environmental Protection 86(6) (2008) 441-447.
[18] B. Freedman, R.O. Butterfield, E.H. Pryde, Transesterification kinetics of soybean oil 1, Journal of the American Oil Chemists' Society 63(10) (1986) 1375-1380.
[19] M. Kalantari, M. Kazemeini, A. Arpanaei, Evaluation of biodiesel production using lipase immobilized on magnetic silica nanocomposite particles of various structures, Biochemical engineering journal 79 (2013) 267-273.
[20] A. Guldhe, B. Singh, T. Mutanda, K. Permaul, F. Bux, Advances in synthesis of biodiesel via enzyme catalysis: Novel and sustainable approaches, Renewable and Sustainable Energy Reviews 41 (2015) 1447-1464.
[21] Y. Yan, X. Li, G. Wang, X. Gui, G. Li, F. Su, X. Wang, T. Liu, Biotechnological preparation of biodiesel and its high-valued derivatives: A review, Applied Energy 113 (2014) 1614-1631.
[22] M.C. Carey, D.M. Small, The characteristics of mixed micellar solutions with particular reference to bile, The American Journal of Medicine 49(5) (1970) 590-608.
[23] A. Svendsen, Lipase protein engineering, Biochimica et Biophysica Acta (BBA)/Protein Structure and Molecular Enzymology 1543(2) (2000) 223-238.
[24] L. Sarda, P. Desnuelle, Action de la lipase pancréatique sur les esters en émulsion, Biochimica et Biophysica Acta 30(3) (1958) 513-521.
[25] P. Reis, K. Holmberg, R. Miller, M.E. Leser, T. Raab, H.J. Watzke, Lipase reaction at interfaces as self-limiting processes, Comptes Rendus Chimie 12(1) (2009) 163-170.
[26] L. Michaelis, M. Menten, Die Kinetik der Invertinwirkung Biochem Z 49: 333–369, (1913).
[27] P. Reis, K. Holmberg, H. Watzke, M. Leser, R. Miller, Lipases at interfaces: a review, Advances in colloid and interface science 147 (2009) 237-250.
[28] I. Panaiotov, M. Ivanova, R. Verger, Interfacial and temporal organization of enzymatic lipolysis, Current opinion in colloid & interface science 2(5) (1997) 517-525.
[29] R. Verger, 'Interfacial activation'of lipases: facts and artifacts, Trends in Biotechnology 15(1) (1997) 32-38.
[30] A. Brzozowski, U. Derewenda, Z. Derewenda, G. Dodson, D. Lawson, J. Turkenburg, F. Bjorkling, B. Huge-Jensen, S. Patkar, L. Thim, A model for interfacial activation in lipases from the structure of a fungal lipase-inhibitor complex, Nature 351(6326) (1991) 491-494.
[31] U. Derewenda, A.M. Brzozowski, D.M. Lawson, Z.S. Derewenda, Catalysis at the interface: the anatomy of a conformational change in a triglyceride lipase, Biochemistry 31(5) (1992) 1532-1541.
[32] P. Grochulski, F. Bouthillier, R.J. Kazlauskas, A.N. Serreqi, J.D. Schrag, E. Ziomek, M. Cygler, Analogs of reaction intermediates identify a unique substrate binding site in Candida rugosa lipase, Biochemistry 33(12) (1994) 3494-3500.

[33] A.M. Brzozowski, H. Savage, C.S. Verma, J.P. Turkenburg, D.M. Lawson, A. Svendsen, S. Patkar, Structural origins of the interfacial activation in Thermomyces (Humicola) lanuginosa lipase, Biochemistry 39(49) (2000) 15071-15082.
[34] A. Brzozowski, Crystallization of a Humicola lanuginosa lipase–inhibitor complex with the use of polyethylene glycol monomethyl ether, Acta Crystallographica Section D: Biological Crystallography 49(3) (1993) 352-354.
[35] M.-P. Egloff, F. Marguet, G. Buono, R. Verger, C. Cambillau, H. van Tilbeurgh, The 2.46. ANG. Resolution structure of the pancreatic lipase-colipase complex inhibited by a C11 alkyl phosphonate, Biochemistry 34(9) (1995) 2751-2762.
[36] A. Roussel, S. Canaan, M.-P. Egloff, M. Rivière, L. Dupuis, R. Verger, C. Cambillau, Crystal structure of human gastric lipase and model of lysosomal acid lipase, two lipolytic enzymes of medical interest, Journal of Biological Chemistry 274(24) (1999) 16995-17002.
[37] A. Roussel, N. Miled, L. Berti-Dupuis, M. Rivière, S. Spinelli, P. Berna, V. Gruber, R. Verger, C. Cambillau, Crystal structure of the open form of dog gastric lipase in complex with a phosphonate inhibitor, Journal of Biological Chemistry 277(3) (2002) 2266-2274.
[38] C.J. O'Connor, P. Walde, Interactions of human milk lipase with sodium taurocholate and other surfactants, Langmuir 2(2) (1986) 139-146.
[39] V. Belle, A. Fournel, M. Woudstra, S. Ranaldi, F. Prieri, V. Thomé, J. Currault, R. Verger, B. Guigliarelli, F. Carrière, Probing the opening of the pancreatic lipase lid using site-directed spin labeling and EPR spectroscopy, Biochemistry 46(8) (2007) 2205-2214.
[40] P. Reis, K. Holmberg, R. Miller, J. Krägel, D.O. Grigoriev, M.E. Leser, H.J. Watzke, Competition between lipases and monoglycerides at interfaces, Langmuir 24(14) (2008) 7400-7407.
[41] M. Cygler, P. Grochulski, R.J. Kazlauskas, J.D. Schrag, F. Bouthillier, B. Rubin, A.N. Serreqi, A.K. Gupta, A structural basis for the chiral preferences of lipases, Journal of the American Chemical Society 116(8) (1994) 3180-3186.
[42] H. Brockerhoff, Substrate specificity of pancreatic lipase, Biochimica et Biophysica Acta (BBA)-Enzymology 159(2) (1968) 296-303.
[43] P. Reis, R. Miller, M. Leser, H. Watzke, V. Fainerman, K. Holmberg, Adsorption of polar lipids at the water− oil interface, Langmuir 24(11) (2008) 5781-5786.
[44] P. Reis, K. Holmberg, R. Miller, J. Krägel, D.O. Grigoriev, M.E. Leser, H.J. Watzke, Competition between Lipases and Monoglycerides at Interfaces, Langmuir 24(14) (2008) 7400-7407.
[45] P. Reis, M. Malmsten, M. Nydén, B. Folmer, K. Holmberg, Interactions between Lipases and Amphiphiles at Interfaces, Journal of Surfactants and Detergents 22(5) (2019) 1047-1058.
[46] P. Reis, H. Watzke, M. Leser, K. Holmberg, R. Miller, Interfacial mechanism of lipolysis as self-regulated process, Biophysical Chemistry 147(3) (2010) 93-103.
[47] R. Verger, F. Pattus, G. Pieroni, C. Riviere, F. Ferrato, J. Leonardi, B. Dargent, Regulation by the “interfacial quality” of some biological activities, Colloids and Surfaces 10 (1984) 163-180.
[48] R. Swisher, Metabolic pathways and ultimate biodegradation, Surfactant biodegradation. Marcel Dekker, New York (1987).
[49] E. Dickinson, Introduction to food colloids, Oxford university press1992.
[50] V. Delorme, R. Dhouib, S. Canaan, F. Fotiadu, F. Carrière, J.-F. Cavalier, Effects of surfactants on lipase structure, activity, and inhibition, Pharmaceutical research 28(8) (2011) 1831-1842.
[51] C.-l. Liu, D.T. Kamei, J.A. King, D.I. Wang, D. Blankschtein, Separation of proteins and viruses using two-phase aqueous micellar systems, Journal of Chromatography B: Biomedical Sciences and Applications 711(1-2) (1998) 127-138.
[52] T. Saitoh, H. Tani, T. Kamidate, H. Watanabe, Phase separation in aqueous micellar solutions of nonionic surfactants for protein separation, TrAC Trends in Analytical Chemistry 14(5) (1995) 213-217.
[53] G. Lye, J. Asenjo, D. Pyle, Protein extraction using reverse micelles: kinetics of protein partitioning, Chemical engineering science 49(19) (1994) 3195-3204.
[54] G. Savelli, N. Spreti, P. Di Profio, Enzyme activity and stability control by amphiphilic self-organizing systems in aqueous solutions, Current opinion in colloid & interface science 5(1-2) (2000) 111-117.
[55] T.E. Creighton, Proteins: structures and molecular properties, Macmillan1993.
[56] R. Schomaecker, B.H. Robinson, P.D. Fletcher, Interaction of enzymes with surfactants in aqueous solution and in water-in-oil microemulsions, Journal of the Chemical Society, Faraday Transactions 1: Physical Chemistry in Condensed Phases 84(12) (1988) 4203-4212.
[57] V.P. Harden, J.O. Harris, The isoelectric point of bacterial cells, Journal of bacteriology 65(2) (1953) 198.

[58] P.P. Polizelli, M.J. Tiera, G.O. Bonilla-Rodriguez, Effect of surfactants and polyethylene glycol on the activity and stability of a lipase from oilseeds of Pachira aquatica, Journal of the American Oil Chemists' Society 85(8) (2008) 749-753.
[59] P. Skagerlind, B. Folmer, B. Jha, M. Svensson, K. Holmberg, Lipase-surfactant interactions, The Colloid Science of Lipids, Springer1998, pp. 47-57.
[60] A. Yonath, A. Podjarny, B. Honig, A. Sielecki, W. Traub, Crystallographic studies of protein denaturation and renaturation. 2. Sodium dodecyl sulfate induced structural changes in triclinic lysozyme, Biochemistry 16(7) (1977) 1418-1424.
[61] D. Otzen, Protein–surfactant interactions: a tale of many states, Biochimica et Biophysica Acta (BBA)-Proteins and Proteomics 1814(5) (2011) 562-591.
[62] B. Folmer, K. Holmberg, M. Svensson, Interaction of Rhizomucor miehei lipase with an amphoteric surfactant at different pH values, Langmuir 13(22) (1997) 5864-5869.
[63] P. Skagerlind, M. Jansson, B. Bergenståhl, K. Hult, Binding of Rhizomucor miehei lipase to emulsion interfaces and its interference with surfactants, Colloids and Surfaces B: Biointerfaces 4(3) (1995) 129-135.
[64] J.E. Mogensen, P. Sehgal, D.E. Otzen, Activation, inhibition, and destabilization of Thermomyces lanuginosus lipase by detergents, Biochemistry 44(5) (2005) 1719-1730.
[65] P. Alam, G. Rabbani, G. Badr, B.M. Badr, R.H. Khan, The surfactant-induced conformational and activity alterations in Rhizopus niveus lipase, Cell biochemistry and biophysics 71(2) (2015) 1199-1206.
[66] P. Skagerlind, K. Holmberg, Effect of the surfactant on enzymatic hydrolysis of palm oil in microemulsion, Journal of dispersion science and technology 15(3) (1994) 317-322.
[67] K. Holmberg, M. Nydén, L.-T. Lee, M. Malmsten, B.K. Jha, Interactions between a lipase and charged surfactants—a comparison between bulk and interfaces, Advances in colloid and interface science 88(1-2) (2000) 223-241.
[68] L.-T. Lee, B.K. Jha, M. Malmsten, K. Holmberg, Lipase− Surfactant Interactions Studied by Neutron Reflectivity and Ellipsometry, The Journal of Physical Chemistry B 103(35) (1999) 7489-7494.
[69] S.S. Magalhaes, L. Alves, M. Sebastiao, B. Medronho, Z.L. Almeida, T.Q. Faria, R.M. Brito, M.J. Moreno, F.E. Antunes, Effect of ethyleneoxide groups of anionic surfactants on lipase activity, Biotechnology progress 32(5) (2016) 1276-1282.
[70] B. Borgstrom, J. Donner, Interactions of pancreatic lipase with bile salts and dodecyl sulfate, Journal of lipid research 17(5) (1976) 491-497.
[71] E. Jurado, V. Bravo, G. Luzón, M. Fernández-Serrano, M. García-Román, D. Altmajer-Vaz, J.M. Vicaria, Hard-surface cleaning using lipases: enzyme–surfactant interactions and washing tests, Journal of Surfactants and Detergents 10(1) (2007) 61-70.
[72] H. Wege, J. Holgado-Terriza, A. Neumann, M. Cabrerizo-Vılchez, Axisymmetric drop shape analysis as penetration film balance applied at liquid–liquid interfaces, Colloids and Surfaces A: Physicochemical and Engineering Aspects 156(1-3) (1999) 509-517.
[73] M. Cabrerizo-Vılchez, H. Wege, J. Holgado-Terriza, A. Neumann, Axisymmetric drop shape analysis as penetration Langmuir balance, Review of scientific instruments 70(5) (1999) 2438-2444.
[74] J.K. Ferri, W.-F. Dong, R. Miller, Ultrathin free-standing polyelectrolyte nanocomposites: a novel method for preparation and characterization of assembly dynamics, The Journal of Physical Chemistry B 109(31) (2005) 14764-14768.
[75] R.A. Ganzevles, K. Zinoviadou, T. van Vliet, M.A. Cohen Stuart, H.H. de Jongh, Modulating surface rheology by electrostatic protein/polysaccharide interactions, Langmuir 22(24) (2006) 10089-10096.
[76] V. Fainerman, R. Miller, J.K. Ferri, H. Watzke, M. Leser, M. Michel, Reversibility and irreversibility of adsorption of surfactants and proteins at liquid interfaces, Advances in colloid and interface science 123 (2006) 163-171.
[77] J.K. Ferri, N. Gorevski, C. Kotsmar, M.E. Leser, R. Miller, Desorption kinetics of surfactants at fluid interfaces by novel coaxial capillary pendant drop experiments, Colloids and Surfaces A: Physicochemical and Engineering Aspects 319(1-3) (2008) 13-20.
[78] A. Javadi, J. Ferri, T.D. Karapantsios, R. Miller, Interface and bulk exchange: Single drops experiments and CFD simulations, Colloids and Surfaces A: Physicochemical and Engineering Aspects 365(1-3) (2010) 145-153.
[79] A. Javadi, M. Karbaschi, D. Bastani, J. Ferri, V. Kovalchuk, N. Kovalchuk, K. Javadi, R. Miller, Marangoni instabilities for convective mobile interfaces during drop exchange: experimental study and CFD simulation, Colloids and Surfaces A: Physicochemical and Engineering Aspects 441 (2014) 846-854.
[80] T. Young, III. An essay on the cohesion of fluids, Philosophical transactions of the royal society of London (95) (1805) 65-87.

[81] P. Laplace, J. Fournier, Sur l'action capillaire. supplément à la théorie de l'action capillaire, Traité de mécanique céleste 4(Supplement 1) (1805) 771-777.
[82] J. Won, V. Ulaganathan, A. Tleuova, T. Kairaliyeva, A. Sharipova, X.W. Hu, M. Karbaschi, G. Gochev, A. Javadi, M.T. Rahni, Profile Analysis Tensiometry for Studies of Liquid Interfacial Dynamics, Laser Optofluidics in Fighting Multiple Drug Resistance (2017) 41-74.
[83] J. Lucassen, M. Van Den Tempel, Dynamic measurements of dilational properties of a liquid interface, Chemical Engineering Science 27(6) (1972) 1283-1291.
[84] R. Miller, L. Liggieri, Interfacial rheology, CRC Press2009.
[85] R. Miller, J.K. Ferri, A. Javadi, J. Krägel, N. Mucic, R. Wüstneck, Rheology of interfacial layers, Colloid and Polymer Science 288(9) (2010) 937-950.
[86] S. Zholob, V. Kovalchuk, A. Makievski, J. Krägel, V. Fainerman, R. Miller, Determination of the dilational elasticity and viscosity from the surface tension response to harmonic area perturbations, Interfacial rheology, Brill Publ.2009, pp. 77-102.
[87] A. Dan, C. Kotsmar, J.K. Ferri, A. Javadi, M. Karbaschi, J. Krägel, R. Wüstneck, R. Miller, Mixed protein–surfactant adsorption layers formed in a sequential and simultaneous way at water–air and water–oil interfaces, Soft Matter 8(22) (2012) 6057-6065.
[88] P. Mukerjee, K.J. Mysels, Critical micelle concentrations of aqueous surfactant systems, National Standard reference data system, 1971.
[89] W. Li, M. Zhang, J. Zhang, Y. Han, Self-assembly of cetyl trimethylammonium bromide in ethanol-water mixtures, Frontiers of Chemistry in China 1(4) (2006) 438-442.
[90] A. Javadi, N. Mucic, D. Vollhardt, V. Fainerman, R. Miller, Effects of dodecanol on the adsorption kinetics of SDS at the water–hexane interface, Journal of colloid and interface science 351(2) (2010) 537-541.
[91] The PyMOL Molecular Graphics System, Version 2.3.5, Schrödinger, LLC.